

# SCIENTIFIC REPORTS



OPEN

## Significance of oxygen transport through aquaporins

Janusz J. Zwiazek<sup>1</sup>, Hao Xu<sup>1</sup>, Xiangfeng Tan<sup>1</sup>, Alfonso Navarro-Ródenas<sup>1,2</sup> & Asunción Morte<sup>2</sup>

Received: 05 October 2016

Accepted: 06 December 2016

Published: 12 January 2017

Aquaporins are membrane integral proteins responsible for the transmembrane transport of water and other small neutral molecules. Despite their well-acknowledged importance in water transport, their significance in gas transport processes remains unclear. Growing evidence points to the involvement of plant aquaporins in CO<sub>2</sub> delivery for photosynthesis. The role of these channel proteins in the transport of O<sub>2</sub> and other gases may also be more important than previously envisioned. In this study, we examined O<sub>2</sub> permeability of various human, plant, and fungal aquaporins by co-expressing heterologous aquaporin and myoglobin in yeast. Two of the most promising O<sub>2</sub>-transporters (*Homo sapiens* AQP1 and *Nicotiana tabacum* PIP1;3) were confirmed to facilitate O<sub>2</sub> transport in the spectrophotometric assay using yeast protoplasts. The over-expression of NtPIP1;3 in yeasts significantly increased their O<sub>2</sub> uptake rates in suspension culture. In *N. tabacum* roots subjected to hypoxic hydroponic conditions, the transcript levels of the O<sub>2</sub>-transporting aquaporin NtPIP1;3 significantly increased after the seven-day hypoxia treatment, which was accompanied by the increase of ATP levels in the apical root segments. Our results suggest that the functional significance of aquaporin-mediated O<sub>2</sub> transport and the possibility of controlling the rate of transmembrane O<sub>2</sub> transport should be further explored.

Since the discoveries that membrane intrinsic proteins (MIPs) are involved in transmembrane water transport<sup>1,2</sup>, evidence has been growing that links different members of the aquaporin family to transport processes of other small neutral molecules, including CO<sub>2</sub><sup>3–5</sup>. The transport of these molecules has been associated with fundamental physiological processes<sup>3,6</sup>. Similarly to the long-prevailing views of water transport, a possible significance of pore-mediated transport for CO<sub>2</sub> and O<sub>2</sub> has been sometimes downplayed due to theoretical and experimental evidence suggesting rapid diffusion of these gases through the lipid bilayer<sup>7,8</sup>. While functional significance of aquaporin-mediated CO<sub>2</sub> transport has been demonstrated for photosynthesis and cell signaling processes<sup>3,6</sup>, the importance of pore-mediated O<sub>2</sub> transport to transcellular O<sub>2</sub> fluxes and cell function remains elusive<sup>9–11</sup>.

In the present study, we used the yeast cell system (*Saccharomyces cerevisiae* INVSc1, Invitrogen) to co-express sperm whale (*Physeter macrocephalus*) myoglobin<sup>12</sup> in the yeast expression vector pAG425GAL-ccdB together with one of the 20 different aquaporins from human, plants, or fungi (Supplementary Information Notes S1 and S2) in the vector pAG426GAL-ccdB, to evaluate the impact of heterologous aquaporin expression on myoglobin oxygenation as an indicator for O<sub>2</sub> permeability of the yeast plasma membrane. We also examined the transcript abundance of plasma membrane intrinsic proteins (PIPs) in relation to ATP levels in the roots of *Nicotiana tabacum* under hypoxia in hydroponic culture in order to evaluate possible functional significance of the O<sub>2</sub>-transporting aquaporins.

### Results

**Protein expression and transcript abundance of myoglobin and aquaporins.** Immunoblotting with anti-myoglobin antibody demonstrated the presence of myoglobin in the selected yeast strains that were constructed to express myoglobin, but not in INVSc1 (Fig. 1A). Quantitative RT-PCR showed that transcript abundance of myoglobin was similar in the transformed yeast strains (Fig. S1). Immunoblotting with anti-human aquaporin 1 antibody demonstrated that the antibody recognized the expressed heterologous aquaporins *Homo sapiens* HsAQP1, *Nicotiana tabacum* NtPIP1;3, and *Arabidopsis thaliana* AtPIP1;2 in the respective strains, and also, weakly, the yeast homologous aquaporins in the mock strain constructed to express myoglobin only (Fig. 1B). The qRT-PCR assay with higher specificity than immunoblotting showed that the transcript abundance

<sup>1</sup>Department of Renewable Resources, University of Alberta, Edmonton, AB, T6G 2E3, Canada. <sup>2</sup>Departamento de Biología Vegetal (Botánica), Facultad de Biología, Universidad de Murcia, Campus de Espinardo, 30100 Murcia, Spain. Correspondence and requests for materials should be addressed to J.J.Z. (email: jzwiazek@ualberta.ca)

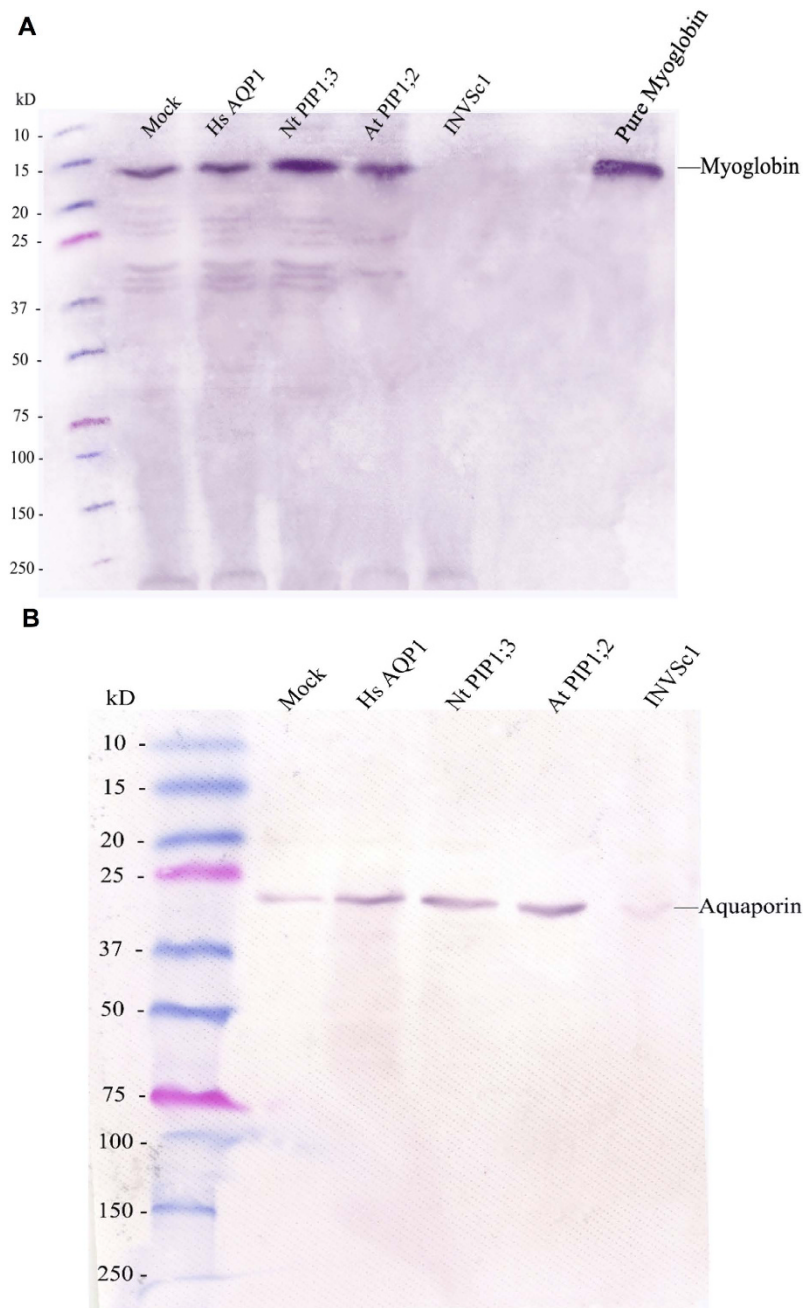


**Figure 1. Immunoblot probed with the anti-myoglobin antibody and the anti-human aquaporin 1 antibody.** (A) The yeast total proteins were immunoblotted with the primary anti-myoglobin antibody. (B) The yeast total proteins were immunoblotted with the primary anti-human aquaporin 1 antibody.

of the heterologously-expressed aquaporin genes *HsAQP1*, *NtPIP1;3* and *AtPIP1;2* was negligible in the mock strain, but significantly high in each corresponding strain (Fig. S1).

Following formaldehyde fixation<sup>13</sup>, paraffin embedding and preparation of sectioned yeast cells for immunodetection with the anti-human aquaporin 1 antibody, strong immunofluorescence was detected in the periphery of the yeast cell section of the *HsAQP1* strain in comparison with the relatively weak intracellular fluorescence signal (Fig. 2), pointing to the plasma membrane as the likely localization site. This is consistent with the subcellular localization prediction by TargetP<sup>14</sup>, suggesting the absence of mitochondrial targeting peptide and pointing to the secretory pathway as the most likely location of *HsAQP1* in eukaryotic cells (Supplementary Information Table S1).

**O<sub>2</sub> transport.** Of the yeast strains that were examined, those expressing *HsAQP1*, *NtPIP1;3*, *NtPIP1;4*, *NtPIP2;1*, and *NtXIP1;1* showed statistically significant increases in O<sub>2</sub> permeability with preliminary spectrophotometric measurements as evidenced by higher rates of change in myoglobin A<sub>541</sub> absorbance (Figs S2 and S3A)

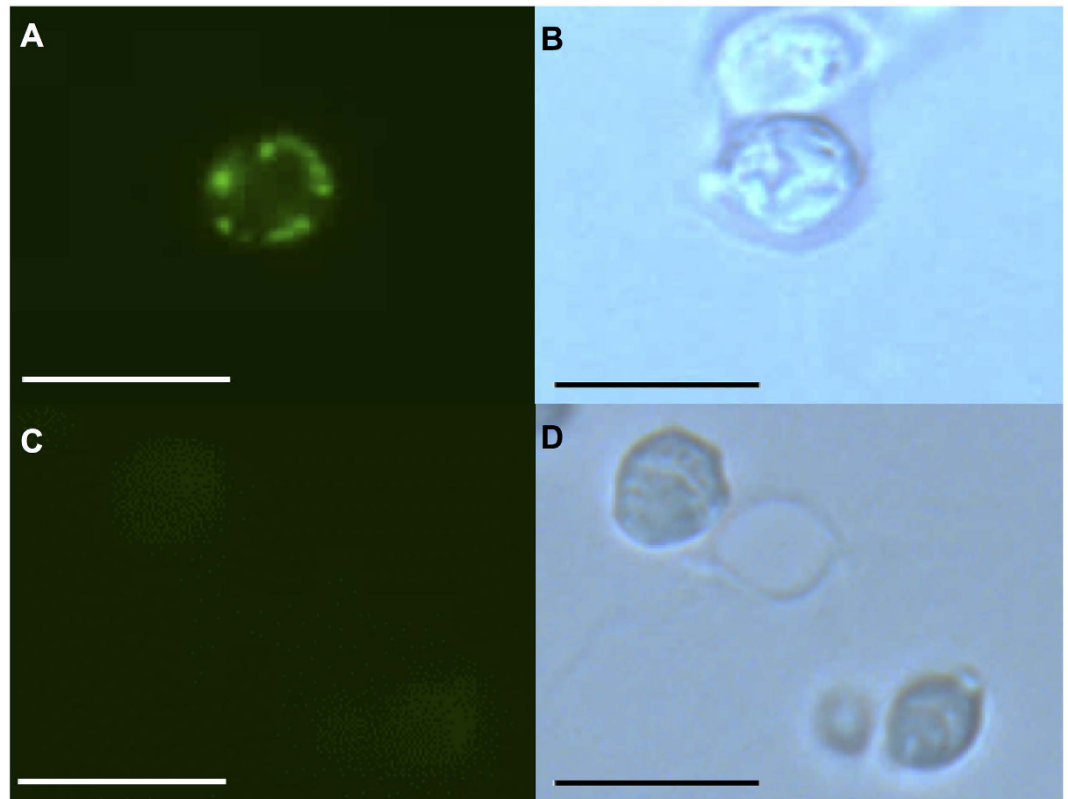


**Figure 2.** Indirect immunofluorescence of paraffin-embedded yeast cells of HsAQP1 strain after the incubation with the primary anti-aquaporin 1 monoclonal antibody and the fluorescein-conjugated secondary antibody. (A) HsAQP1 strain under blue light excitation. (B) HsAQP1 strain in bright field. (C) Mock strain under blue light excitation. (D) Mock strain in bright field. The length of bars is 10  $\mu\text{m}$ .

compared with mock control (Fig. S3B). Over-expression of the *A. thaliana* (AtPIP1;1, AtPIP1;2, AtPIP1;3, AtPIP1;4, and AtPIP2;1) and *Laccaria bicolor* (LbAQP1, LbAQP3, LbAQP5, LbAQP6, and LbAQP7) aquaporins did not alter  $A_{541}$  absorbance (Fig. S3B), indicating no significant effect on  $\text{O}_2$  permeability.

Two of the most promising  $\text{O}_2$ -transporters (HsAPQ1 and NtPIP1;3) and one that did not show  $\text{O}_2$ -transporting properties in preliminary experiments (AtPIP1;2), as well as the mock strain were further analyzed in yeast protoplast assay. Based on the spectrum scanning on purified myoglobin (Fig. S2) and yeast protoplasts (Fig. S4),  $\Delta A_{541}/\Delta A_{600}$  and  $\Delta A_{319}/\Delta A_{341}$  (Fig. S5) were chosen to indicate myoglobin oxygenation.  $\Delta A_{541}/\Delta A_{600}$  at 90 s showed the same trend across the strains with the preliminary assay: the strain expressing NtPIP1;3 had the highest value, followed by HsAQP1, mock and AtPIP1;2 in order (Fig. 3).  $\Delta A_{319}/\Delta A_{341}$  after 5 min with 5 times of 30 s aeration demonstrated more distinct statistical difference between HsAQP1 and mock, and between all of the myoglobin-expressing strains and untransformed strain INVSc1 (Fig. 4).

Since the conversion of deoxymyoglobin to oxymyoglobin is iron-dependent, and may be affected by the cell redox status, the redox state of selected strains after being pretreated for  $\text{O}_2$  transport assay was measured using CM- $\text{H}_2\text{DCFDA}$ . Fluorescence intensity generated by CM- $\text{H}_2\text{DCFDA}$  showed no significant difference between yeast strains after the pretreatment of  $\text{O}_2$  transport assay (Fig. S6). This suggested that the cell redox state in the mock, HsAQP1, NtPIP1;3 and AtPIP1;2 strains was similar prior to the  $\text{O}_2$  transport assay. Similarly to the earlier report<sup>6</sup>, increased  $\text{H}_2\text{O}_2$  permeability was detected in NtPIP1;2 strain (Fig. S7). However, no increase in  $\text{H}_2\text{O}_2$  permeability was measured in NtPIP1;3, HsAQP1 or mock strains, whereas a slightly higher fluorescence intensity suggesting increased  $\text{H}_2\text{O}_2$  permeability in AtPIP1;2 strain was not statistically significant (Fig. S7).

**Yeast  $\text{O}_2$  consumption capacity.** Yeast cells heterologously expressing NtPIP1;3 and HsAQP1 showed 2.3-fold and 1.8-fold higher  $\text{O}_2$  uptake rates, respectively, compared with mock control (Fig. 5A) and depleted oxygen from the solution significantly faster ( $P \leq 0.05$ ) (Figs 5B and S8). The  $\text{O}_2$  uptake rates of yeast cells expressing AtPIP1;2 and the time for  $\text{O}_2$  depletion from the solution were not significantly ( $P \geq 0.05$ ) different from the mock controls (Fig. 5). Yeast cell diameter was not significantly affected by the heterologous expression of aquaporins and measured  $2.87 \pm 0.05$ ,  $2.74 \pm 0.06$ ,  $2.98 \pm 0.06$ , and  $2.87 \pm 0.08 \mu\text{m}$  (mean,  $n = 50 \pm \text{SE}$ ) in mock, HsAQP1, NtPIP1;3, and AtPIP1;2 strains.

**PIP transcript abundance and ATP level in tobacco roots under hypoxia.** We examined transcript levels of tobacco plants subjected to flooding-induced hypoxia in mineral solution culture for two and seven days. After two days of hypoxia ( $\approx 125 \mu\text{mol L}^{-1} \text{O}_2$ ), leaf and root transcript levels of NtPIP1;3 (the aquaporin showing

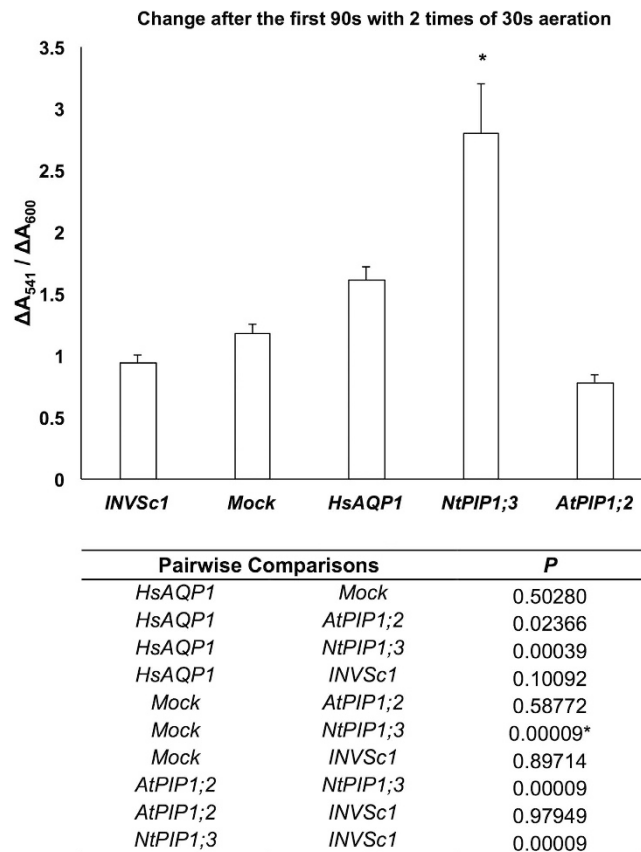


**Figure 3.**  $\Delta A_{541}/\Delta A_{600}$  of yeast protoplasts after the first 90 s with 2 times of 30 s aeration. Asterisks indicate statistically significant difference with the mock strain ( $P$  values shown in the table below) (ANOVA, Tukey's test,  $P \leq 0.05$ ,  $n = 19 \pm SE$ ).

the high rate of  $O_2$  transport) increased by about four-fold compared with well-aerated ( $\approx 500 \mu\text{mol L}^{-1} O_2$ ) plants (Fig. 6A,B). In well-aerated plants, aquaporin transcript levels remained similar on days two and seven in leaves and roots (Fig. 6A–D). Relatively minor increases were also measured for transcript levels of *NtPIP1;4* in leaves and *NtPIP1;1* and *NtPIP1;2* in roots (Fig. 6A,B). After seven days, a sharp increase of *NtPIP1;3* was measured in hypoxic leaves (about 12-fold higher than aerated control) and roots (about 22-fold higher than aerated control) (Fig. 6C,D). There was also about three-fold increase in *NtPIP2;1* in the leaves (Fig. 6C). Under the hypoxia treatment, from day two to day seven, the *NtPIP1;3* transcript levels sharply increased in both leaves ( $P = 0.0001$ ) and roots ( $P = 0.0037$ ) (Fig. 6), which was accompanied by a significant increase in ATP levels in the apical root segments (Fig. 7;  $P = 0.0267$ ). After seven days of treatment, hypoxic and well-aerated roots had similar ATP levels in each root segment (Fig. 7B). Hypoxic plants showed healthy and green appearance, without chlorosis or other visible signs of  $O_2$  deficiency.

## Discussion

In this study, we investigated the potential contribution of aquaporins to transmembrane  $O_2$  transport in yeast whole cells and yeast protoplasts by measuring absorbance near the peak wavelengths of myoglobin over time. In the whole-cell assay,  $A_{541}$  increased over the first 60 s, which enabled us to screen strains that expressed putative  $O_2$ -transporting aquaporins (Fig. S3B). Changes in  $A_{541}$  likely represent a combination of several processes including  $O_2$  diffusion, oxygenation of deoxymyoglobin, conversion between oxymyoglobin and metmyoglobin, and  $O_2$  consumption. The presence of cell walls might hinder the changes in absorbance in myoglobin and lead to an underestimation of  $O_2$  diffusion in the preliminary screening. In addition, possible artifacts on absorbance reading might be caused during the mixing of the yeast suspension and aerated buffer. The yeast protoplast assay aimed to eliminate these potential pitfalls with numerous precautions and more replications and to maximize the signal of myoglobin oxygenation. The results suggested that  $\Delta A_{319}/\Delta A_{341}$  in yeast protoplast assay may also be a highly sensitive parameter in measuring  $O_2$  transport through aquaporins.

Human aquaporin HsAQP1, which we found to enhance myoglobin oxygenation by facilitating  $O_2$  passage, was also reported to facilitate  $CO_2$  transport when heterologously expressed in *Xenopus laevis* oocytes<sup>15</sup>. However, other major  $CO_2$ -transporting aquaporins including *AtPIP1;2*<sup>5</sup>, *NtPIP1;2*<sup>3</sup> and *LbAQP1*<sup>6</sup> did not facilitate  $O_2$  transport when expressed in yeast (Fig. S3B). This suggests that aquaporin orthologues have developed certain degree of specificity for  $O_2$  transport. The alignment of all the 20 analyzed aquaporins does not show consensus residues that are exclusive to  $O_2$ -transporting aquaporins (Note S3). It appears that the conserved residues

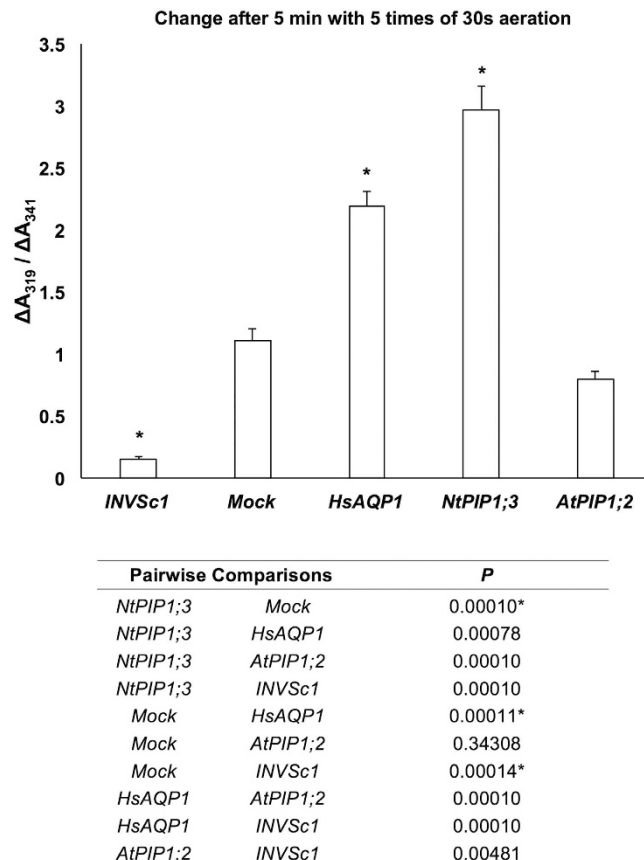


**Figure 4.**  $\Delta A_{319}/\Delta A_{341}$  of yeast protoplasts after 5 min with 5 times of 30 s aeration. Asterisks indicate statistically significant difference with the mock strain ( $P$  values shown in the table below) (ANOVA, Tukey's test,  $P \leq 0.05$ ,  $n = 6 \pm SE$ ).

are species-dependent rather than being relevant to transport capacity. However, it is noteworthy that all six  $O_2$ -transporting aquaporins have well-conserved 29 amino acid residues across species, including most of the Asn-Pro-Ala (NPA) signature motifs and the selective filters of Ar/R residues (Note S4). In *NtPIP1;3*, the asparagine residue commonly in the second NPA motif is substituted by threonine (Thr-235), which may be potentially relevant to its highly enhanced  $O_2$ -transporting capacity.

Calculations of permeation of hydrophobic gases ( $O_2$ ,  $CO_2$ , and  $NO$ ) have consistently shown similar values of an energy barrier of 5–6 kcal mol<sup>-1</sup> through water pores<sup>16,17</sup>. Membrane protein simulation systems of the human *HsAQP1* tetramer have demonstrated the presence of a pore located in the center between the four monomers that is lined by largely hydrophobic residues and may be involved in the transport of gases rather than water<sup>16,18</sup>. It could be speculated that the presence and the exact structure of this pore imparts gas transport specificity to different aquaporins. In proven correct, the gating properties of this pore could be targeted to alter rates of the transmembrane passage of gases.

The results of yeast  $O_2$  uptake rate corroborate those of the  $O_2$  transport assays, pointing to the significance of pore-mediated transport for respiration. Increased transcript levels of *HsAQP1*, also sometimes accompanied by other aquaporins, have been commonly reported for cancerous cells<sup>19,20</sup>, with the level of *HsAQP1* expression often correlated with cell growth, grade of tumor<sup>20,21</sup>, and metastasis<sup>22,23</sup>. It has been also reported that the deletion of *HsAQP1* was effective in reducing breast tumor size and lung metastasis<sup>23</sup> and *HsAQP1* silencing inhibited the proliferation and invasiveness of osteosarcoma cells<sup>24</sup>. Although the proposed explanations for the links between *HsAQP1* expression and cancerous growth have largely focused on water transport, the association between high  $O_2$  demand of rapidly growing cancerous cells and facilitation of  $O_2$  transport by *HsAQP1* should also be considered.

Since the reports of hypoxia-induced expression of *HsAQP1*<sup>25,26</sup> suggest that aquaporin-mediated transport processes may be especially important under low- $O_2$  conditions, we examined transcript levels of *N. tabacum* plants subjected to flooding-induced hypoxia. Although the ATP levels showed some decline in well-aerated plants after 7 days compared with 2 days (Fig. 7A,B), the reverse trend was observed in plants subjected to root hypoxia resulting in similar ATP levels in leaves and all root segments of hypoxic and well-aerated plants after 7 days of hypoxia (Fig. 7A,B). The results suggest that after the initial hypoxic stress, plants likely received sufficient oxygen to support aerobic respiration, as hypoxic plants had healthy and green appearance and did not show chlorosis or other visible signs of  $O_2$  deficiency. While the resistance to root hypoxia can be explained in some plants by an increased supply of  $O_2$  to the root cells through the development of specialized aerating structures

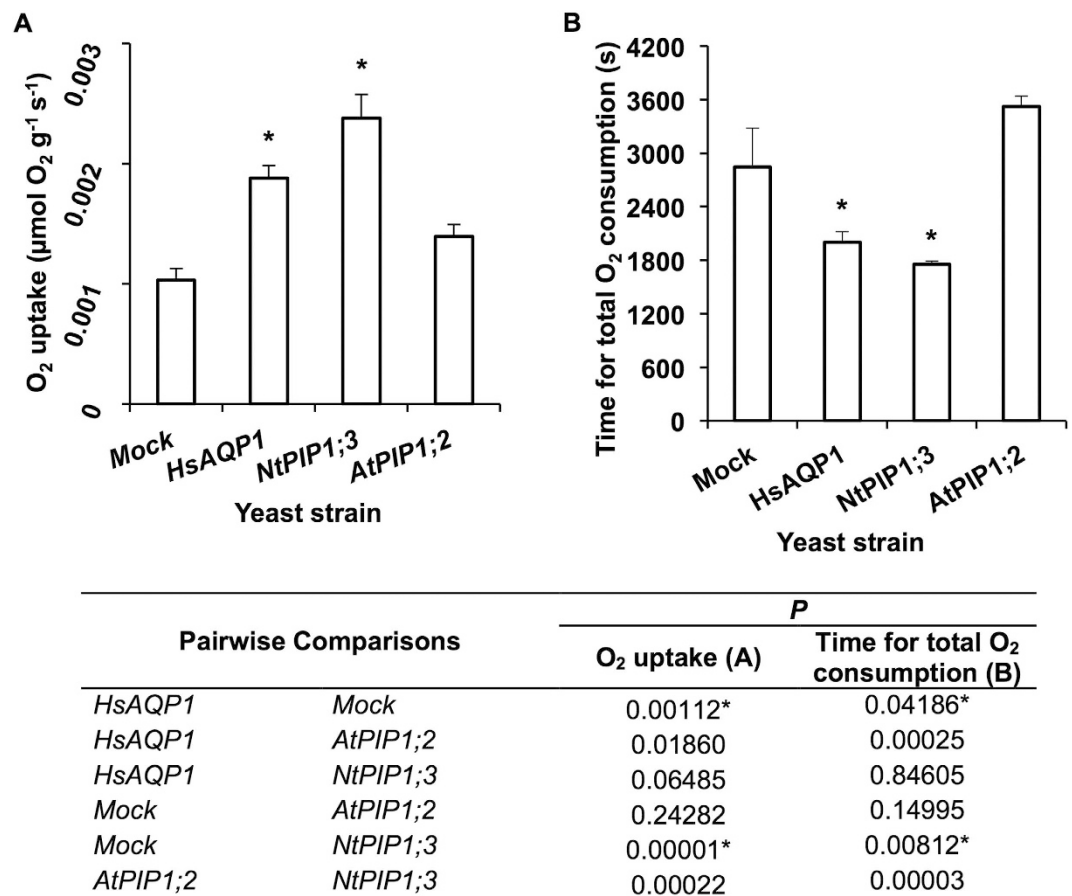


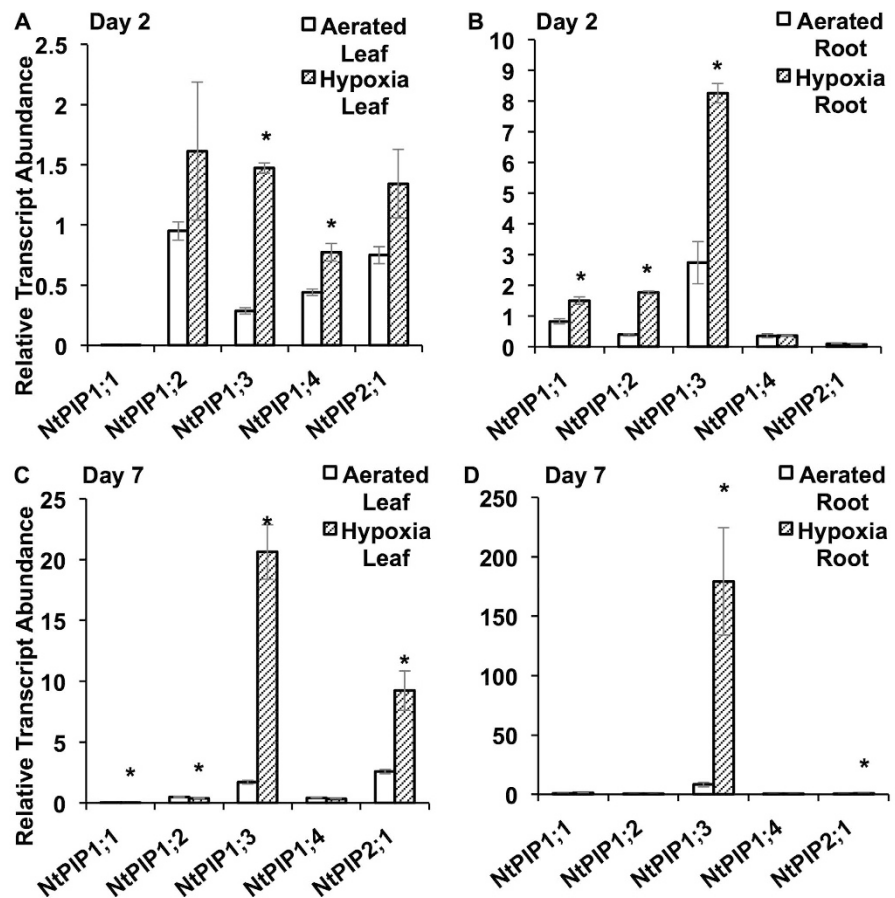
**Figure 5.** O<sub>2</sub> consumption of yeast strains over 1000 s. (A) Respiration rates in *HsAQP1*, *NtPIP1;3*, *AtPIP1;2*, and mock strain (control). (B) Time for total O<sub>2</sub> consumption in *HsAQP1*, *NtPIP1;3*, *AtPIP1;2*, and mock strain (control). Immediately after air was supplied to the yeast suspension in N<sub>2</sub>-bubbled SD-L-U + glucose medium to reach the saturation concentration of soluble O<sub>2</sub> of 235 μmol L<sup>-1</sup>, the decrease of O<sub>2</sub> concentration in yeast suspension was monitored and logged per second using an O<sub>2</sub> microsensor. Asterisks indicate statistically significant difference with the mock strain (*P* values shown in the table below) (ANOVA, Tukey's test, *P* ≤ 0.05, *n* = 6 ± SE).

such as aerenchyma, the processes of plant resistance to hypoxia in the absence of obvious structural changes remain obscure. In our study, there were no structural features present in the roots and stems of plants exposed to root hypoxia that could be indicative of improved O<sub>2</sub> delivery. Therefore, the increase in *NtPIP1;3* transcript levels (Fig. 6) could be among important factors contributing to improved root aeration, similarly to the increased transcript levels of *HsAQP1* in hypoxic human tissues<sup>25,26</sup>. Clearly, the link between pore-mediated O<sub>2</sub> transport and hypoxia deserves further attention.

In conclusion, our results indicate that some of the studied plant and human aquaporins are likely to be involved in O<sub>2</sub> transport. Yeast cells heterologously expressing these aquaporins maintained higher O<sub>2</sub> uptake rates in liquid culture and tobacco plants exhibited sharp increases in the putative O<sub>2</sub>-transporting aquaporin after their roots were subjected to hypoxic conditions. These increases in O<sub>2</sub> transporting aquaporins after the seven-day hypoxia treatment were accompanied by increases in ATP levels in hypoxic apical root segments. The results of the study support the notion that functional significance of pore-mediated O<sub>2</sub> transport should receive more attention.

## Methods

**Expression of myoglobin and aquaporins in yeast.** The complete ORF of sperm whale (*Physeter macrocephalus*) myoglobin (NCBI accession number J03566.1) was sub-cloned from pMB413<sup>12</sup> into the yeast expression vector pAG425GAL-ccdB (<http://www.addgene.org/yeast-gateway/>), by the Gateway technology (Invitrogen, Carlsbad, CA, USA). The complete ORFs of the 20 aquaporin genes of interest were sub-cloned from pGEM-T Easy into the yeast expression vector pAG426GAL-ccdB (<http://www.addgene.org/yeast-gateway/>), by the same method, respectively. These genes include three animal aquaporins from *Homo sapiens* - *HsAQP1* (DQ895575), *HsAQP2* (CR542024) and *HsAQP3* (CR541991), 12 plant aquaporins - *NtPIP1;1* (AF440271), *NtPIP1;2* (AF024511), *NtPIP1;3* (U62280), *NtPIP1;4* (DQ914525), *NtPIP2;1* (AF440272) and *NtXIP1;1* (HM475294) from *Nicotiana tabacum*, and *AtPIP1;1* (AT3G61430), *AtPIP1;2* (AT2G45960), *AtPIP1;3* (AF348574), *AtPIP1;4* (AT4G00430), *AtPIP1;5* (AT4G23400) and *AtNIP2;1* (AT2G34390) from *Arabidopsis*



		Pairwise Comparisons		P value				
				NtPIP1;1	NtPIP1;2	NtPIP1;3	NtPIP1;4	NtPIP2;1
Leaf	Day 2 (A)	Aerated	Hypoxia	0.46632	0.27901	0.00014*	0.00182*	0.07029
	Day 7 (C)	Aerated	Hypoxia	0.01783*	0.03779*	0.00015*	0.08806	0.00232*
	Aerated	Day 2	Day 7	0.00344	0.00029	0.00014	0.58750	0.00014
	Hypoxia	Day 2	Day 7	0.06838	0.05708	0.00014	0.00045	0.00083
Root	Day 2 (B)	Aerated	Hypoxia	0.00157*	0.00014*	0.00015*	0.88071	0.10214
	Day 7 (D)	Aerated	Hypoxia	0.17920	0.75264	0.00368*	0.62456	0.01083*
	Aerated	Day 2	Day 7	0.76947	0.45999	0.02618	0.79194	0.00023
	Hypoxia	Day 2	Day 7	0.12147	0.00014	0.00367	0.53097	0.00162

**Figure 6.** Transcript abundance of tobacco plasma membrane intrinsic proteins (PIPs) after exposure to well-aerated and hypoxic conditions. Relative transcript abundance of selected PIPs in (A) leaves and (B) roots after 2 days of exposure, and in (C) leaves and (D) roots after 7 days of exposure. Transcript abundance of PIPs was measured by the standard curve method in qRT-PCR assay, with normalization against geometric mean of that of the two reference genes, *EF1- $\alpha$*  and *L25*. Asterisks indicate significance difference in gene expression between well-aerated and hypoxic treatments on the same day; *P* values for the comparisons between day two and day seven are listed in the table below (ANOVA, Tukey's test,  $P \leq 0.05$ ,  $n = 6 \pm SE$ ).

*thaliana*, and five fungal aquaporins from *Laccaria bicolor* – *LbAQP1* (JQ585592), *LbAQP3* (JQ585593), *LbAQP5* (JQ585594), *LbAQP6* (JQ585595) and *LbAQP7* (JQ585596). The constructs were verified using primer GAL1 (AATATACCTCTATACTTTAACGTC) in Sanger sequencing. *Saccharomyces cerevisiae* strain INVSc1 (MATA his3D1 leu2 trp1-289 ura3-52; Invitrogen) was double-transformed with pAG425GAL-ccdB + myoglobin vector and one of the PAG426GAL-ccdB + aquaporin vectors, following the protocol of small-scale yeast transformation (Invitrogen). For mock control, INVSc1 was transformed with pAG425GAL-ccdB + myoglobin vector and empty PAG426GAL-ccdB vector.

Selection was based on *ura3* and *leu2* complementation. Transformed yeasts were cultured in glucose containing synthetic complete medium without Ura/Leu (United States Biological) (2 g of yeast nitrogen base, 2 g of dropout amino acids, 5 g of  $(NH_4)_2SO_4$ , 30 g of glucose in 1 L of SD-L-U + glucose medium, pH = 6) for 24 h at  $1.2 \times g$  and 30 °C. Cultures were diluted to an optical density of  $OD_{600} = 0.6$ . Heterologous protein expression was induced by changing the carbon source of the medium from glucose to galactose (30 g in 1 L

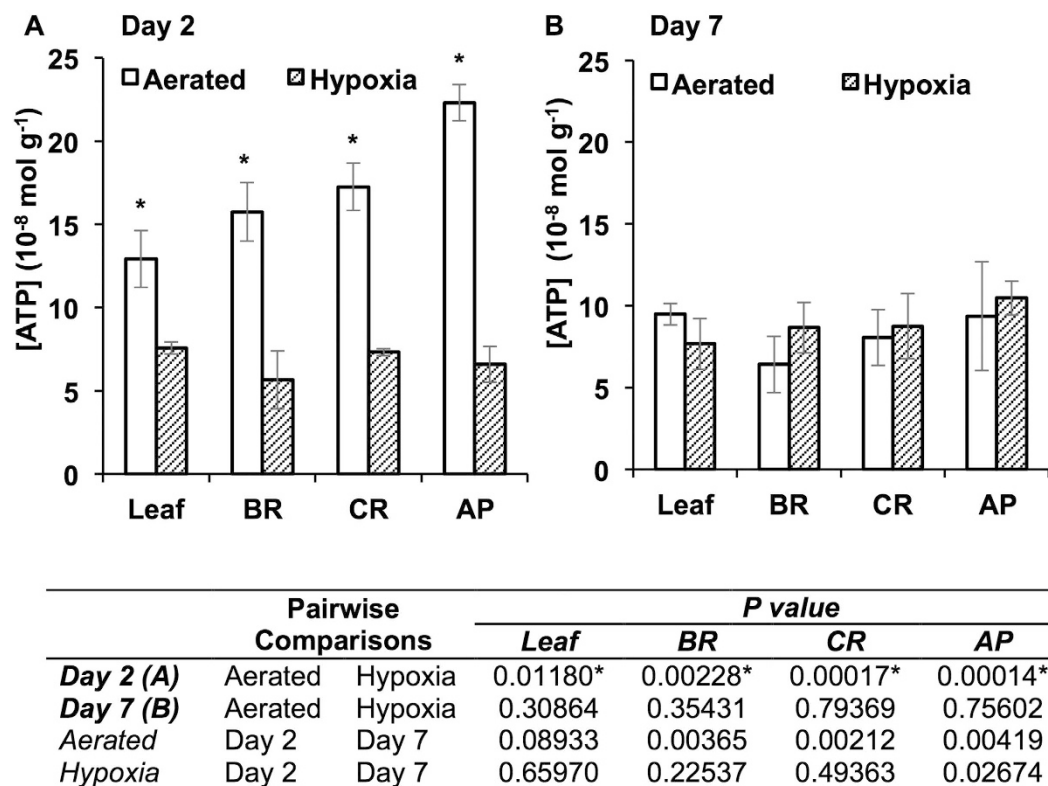


**Figure 7.** ATP levels in leaves and basal (BR), central (CR) and apical (AP) root segments of tobacco plants subjected to hypoxic and well-aerated conditions. (A) ATP levels after 2 days of the treatments. (B) ATP levels after 7 days of the treatments. ATP level was determined by detecting bioluminescence in Luciferase/Luciferin reaction. Asterisks indicate significant differences in ATP levels between well-aerated and hypoxic treatments in the same tissue on the same day; *P* values for the comparisons between day two and day seven are listed in the table below (ANOVA, Tukey's test,  $P \leq 0.05$ ,  $n = 6 \pm SE$ ).

of SD-L-U + galactose medium) and growing yeast cells for 24 h ( $1.2 \times g$ ,  $30^\circ C$ ), with  $25 \text{ mg L}^{-1} \text{ FeSO}_4$  as iron source to promote the formation of myoglobin-iron binding structure<sup>27</sup>, validated by transcript abundance assay of quantitative RT-PCR<sup>28,29</sup> (Method S1), immunoblotting (Method S2) and indirect immunofluorescence detection (Method S3).

**O<sub>2</sub> Transport Assay.** The yeasts were washed in  $\text{KH}_2\text{PO}_4$  buffer (0.1 M, pH 6) twice, and then suspended in  $\text{N}_2$ -bubbled  $\text{KH}_2\text{PO}_4$  buffer. The yeast suspension was bubbled with  $\text{N}_2$  for 30 s and vacuumed for 30 min, to minimize the soluble  $\text{O}_2$  in yeast suspension, which is crucial to maintain the state of deoxymyoglobin<sup>30,31</sup>. The spectrum between 500 nm and 600 nm of yeast suspension was scanned after  $\text{O}_2$  depletion and re-aeration. Compared to the spectrum of purified myoglobin<sup>31</sup>, the spectrum of yeast suspension suggests that the state of metmyoglobin was likely dominant over deoxymyoglobin and oxymyoglobin. In addition, the absorbance spectrum of yeast cell suspension is expectably more complex than purified myoglobin proteins. Despite these limitations, the change in  $A_{541}$  after re-aeration was noticeable (Fig. S3A), which was in the range of 541–543 nm, i.e., the absorption peak of purified oxymyoglobin in the study of Zhao *et al.*<sup>30</sup> as well as in our observation (Fig. S2). The increase in  $A_{541}$  reflects the conversion of deoxymyoglobin into the oxygenated state upon  $\text{Fe}^{2+}$ - $\text{O}_2$  binding, which can be attributed to  $\text{O}_2$  influx. The rate of increase in  $A_{541}$  ( $\Delta A_{541} \text{ s}^{-1}$ ) can reflect the capacity of  $\text{O}_2$  uptake by the yeast strains expressing different aquaporins. Therefore, absorbance of 1 mL yeast suspension of each strain was recorded at 541 nm for 2 min at 1 s interval immediately after the addition of 1 mL of air-saturated  $\text{KH}_2\text{PO}_4$  buffer or  $\text{N}_2$ -saturated  $\text{KH}_2\text{PO}_4$  as negative control, respectively, using a spectrophotometer (Thermo Genesys 10S V4.002, ThermoFisher Scientific). All measurements were carried out at  $22^\circ C$ . The mean and standard error were calculated based on six biological replications. CM- $\text{H}_2\text{DCFDA}$ <sup>32</sup> was used to indicate oxidative state of selected yeast strains due to such pretreatment and to determine  $\text{H}_2\text{O}_2$  transport capacity of selected aquaporins<sup>33</sup> (Methods S4).

After screening the strains that expressed putative  $\text{O}_2$ -transporting aquaporins by measuring the increase in  $A_{541}$  over 60 s with the spectrophotometer (Fig. S3B), yeast protoplasts were prepared for the selected ones for the refined  $\text{O}_2$  transport assay. After induction, 4 mL of yeast culture at  $\text{OD}_{600} = 2$  of each strain was harvested, pre-incubated, washed and treated with zymolyase (Yeast lyticase 100T, United States Biological) at  $37^\circ C$ , 50 rpm for 2 hr. Yeast protoplasts were re-suspended in 10 mL of enzyme buffer (1.2 M sorbitol, 50 mM magnesium acetate, 10 mM  $\text{CaCl}_2$  in autoclaved deionized distilled water). For the initial  $\text{O}_2$ -depleted state, the absorbance spectrum was scanned from 300 nm to 650 nm immediately after mixing 500  $\mu\text{L}$  of protoplast suspension

with 500  $\mu\text{L}$  of isosmotic sodium ascorbate buffer (0.6 M sodium ascorbate, 50 mM magnesium acetate, 10 mM  $\text{CaCl}_2$  in autoclaved deionized distilled water). Sequential scanning was conducted after each 30 s of direct aeration at time points of 30 s, 90 s, 150 s and every minute up to the 10<sup>th</sup> min. At 541–543 nm, myoglobin of the oxygenated state has a pronounced absorbance peak<sup>31</sup> (Fig. S2). At 319–330 nm, both myoglobin (Fig. S2) and myoglobin-expressing yeast protoplasts showed a second, much more pronounced absorbance peak in the oxygenated state (Fig. S4B–E), which was absent in untransformed yeast strain (Fig. S4A). The value of  $A_{319}/A_{341}$  increased dramatically along with multiple aeration (Fig. S5C), suggesting  $\Delta A_{319}/\Delta A_{341}$  be a good indicator for myoglobin oxygenation. Therefore, both  $\Delta A_{541}/\Delta A_{600}$  and  $\Delta A_{319}/\Delta A_{341}$  were calculated to present the change in absorbance due to myoglobin oxygenation. Statistically significant difference across all the strains was analyzed in  $\Delta A_{541}/\Delta A_{600}$  of yeast protoplasts at 90 s (ANOVA, Tukey test,  $P \leq 0.05$ ,  $n = 19$ ;  $P$  values shown in the table of Fig. 3) and in  $\Delta A_{319}/\Delta A_{341}$  after 5 min with 5 times of 30 s aeration (ANOVA, Tukey test,  $P \leq 0.05$ ,  $n = 6$ ;  $P$  values are shown in the table of Fig. 4).

For spectrum scanning of myoglobin, purified horse myoglobin protein at 1 mg/mL was mixed with 1 volume of 10% sodium ascorbate to generate the deoxygenated state, followed by the above-mentioned series of aeration to achieve the state of oxymyoglobin.

**Oxygen uptake by yeast.**  $\text{O}_2$  uptake rates in yeast suspension culture were continuously monitored over 40 min in the over-expression and mock strains (Fig. S8). The time required for the yeast suspension cultures to deplete  $\text{O}_2$  from the solution was also measured, with glucose as a carbon source. *S. cerevisiae* strains INVSC1 for the expression of HsAQP1, or NtPIP1;3, or AtPIP1;2, and the mock control strain, were cultured and induced for heterologous protein expression as described above. The yeasts were washed in  $\text{KH}_2\text{PO}_4$  buffer (0.1 M, pH 6) twice, and then suspended in 15 mL of  $\text{N}_2$ -bubbled SD-L-U + glucose medium in 50 mL Falcon tubes to reach  $\text{OD}_{600} = 5$ . Air was supplied into the yeast suspension until its concentration of soluble  $\text{O}_2$  reached about 235  $\mu\text{mol L}^{-1}$ , the stable saturation level of the still medium at 25 °C. Starting from this point, the decrease of  $\text{O}_2$  concentration in yeast suspension was monitored and logged per second using an  $\text{O}_2$  microsensor with tip diameter of 50  $\mu\text{m}$  (OX-50) connected to the OXY-Meter, a compact  $\text{O}_2$  microsensor amplifier (Unisense, Aarhus, Denmark). Parafilm was used to seal and minimize free air diffusion to the Falcon tubes. The slopes of the decline in  $\text{O}_2$  concentration during the initial 0–1000 s were calculated by linear regression, in which absolute values represented the rates of  $\text{O}_2$  consumption by different yeast strains during the corresponding intervals.  $\text{O}_2$  depletion time of each yeast suspension was recorded. The means and standard errors were calculated based on six biological replications.

**Tobacco Root Hypoxia Study: Growth Conditions and Treatment.** Tobacco (*Nicotiana tabacum L.*) seeds were germinated in soil and plants grown for two weeks in a controlled-environment growth room maintained at 22/18 °C (day/night) temperatures, 60  $\pm$  10% relative humidity, and 18-h photoperiod with photosynthetic photon flux density of approximately 350  $\mu\text{mol m}^{-2} \text{s}^{-1}$ . After two weeks of growth, plants were transferred to containers with half-strength modified Hoagland's solution aerated with aquarium pumps (dissolved  $\text{O}_2$  of approximately 7.5 mg  $\text{L}^{-1}$ ). Thirty-six plants were randomly placed in six containers. After one week, the plants in three containers were subjected to hypoxia by flushing water with nitrogen gas to reach a dissolved  $\text{O}_2$  level of 2 mg  $\text{L}^{-1}$ , and then left stagnant. The plants in the other three containers continued to be aerated.

**Quantitative RT-PCR in tobacco.** Roots and leaves were sampled after two and seven days of hypoxia treatment ( $n = 6$ ). The tissue samples were frozen and homogenized in liquid nitrogen using mortar and pestle. Total RNA was extracted using RNeasy Plant Mini Kit (Qiagen, Valencia, CA, USA). The cDNA synthesis and qPCR were conducted as described in Method S1. The transcript abundance of *NtPIP1;1*, *PIP1;2*, *PIP1;3*, *PIP1;4* and *PIP2;1* was normalized against geometric mean of that of the two reference genes, *EF1- $\alpha$*  and ribosomal protein *L25*. Gene-specific primers were designed using Primer Express 3.0 (Applied Biosystems, Life Technologies) (Table S2).

**Determination of ATP Level.** ATP levels were measured in leaves and apical, central and basal root segments after 2 and 7 days of hypoxia and in well-aerated plants. Roots and leaves of tobacco were sampled after two and seven days of treatments. The roots were divided into the basal, apical and central segments. Tissue samples were ground and 50 mg ground samples were placed in 600  $\mu\text{L}$  of ice-cold 5% Trichloroacetic acid (TCA)<sup>34</sup> in 2 mL centrifuge tubes. The samples were vigorously vortexed for 20 s, left on ice for 10 min and centrifuged at 10,000  $\times g$ , 4 °C for 10 min. Each 400  $\mu\text{L}$  of supernatant was collected and added to 400  $\mu\text{L}$  of ice-cold Tris-acetate buffer (pH = 7.75, 1 M). For the ATP assay, 4  $\mu\text{L}$  of the mixture was pipetted into 96  $\mu\text{L}$  of ATP-free water into a well of the 96-well plate (Costar 96 well plate with flat bottom). To quantify ATP, 50  $\mu\text{L}$  of rLuciferase/Luciferin reagent from ENLITEN ATP Assay Kit (Promega, Madison, WI, USA) was added into each well, and the standard curve was prepared following the manufacturer's protocol. Bioluminescence signal<sup>35</sup> was detected using a microplate reader (Fluostar Optima, BMG Labtech, Ortenberg, Germany).

**Statistical Analysis.** The means and standard errors were calculated based on the biological replications in each assay by descriptive statistics. Statistical difference was analyzed using one-way ANOVA (Tukey's test,  $P \leq 0.05$ ).

## References

- Benga, G., Popescu, O., Pop, V. I. & Holmes, R. p-(Chloromercuri)benzenesulfonate binding by membrane proteins and the inhibition of water transport in human erythrocytes. *Biochemistry* **25**, 1535–1538 (1986).
- Agre, P. et al. Aquaporin CHIP: the archetypal molecular water channel. *Am. J. Physiol.* **265**, F463–476 (1993).
- Uehlein, N., Lovisolio, C., Siefritz, F. & Kaldenhoff, R. The tobacco aquaporin NtAQP1 is a membrane  $\text{CO}_2$  pore with physiological functions. *Nature* **425**, 734–737 (2003).

4. Navarro-Ródenas, A., Ruíz-Lozano, J. M., Kaldenhoff, R. & Morte, A. The aquaporin TcAQP1 of the desert truffle *Terfezia claveryi* is a membrane pore for water and CO<sub>2</sub> transport. *Mol. Plant Microbe In.* **25**, 259–266 (2012).
5. Uehlein, N., Sperling, H., Heckwolf, M. & Kaldenhoff, R. The Arabidopsis aquaporin PIP1; 2 rules cellular CO<sub>2</sub> uptake. *Plant Cell Environ.* **35**, 1077–1083 (2012).
6. Navarro-Ródenas, A., Xu, H., Kemppainen, M., Pardo, A. G. & Zwiazek, J. J. *Laccaria bicolor* Aquaporin LbAQP1 is required for Hartig net development in trembling aspen (*Populus tremuloides*). *Plant Cell Environ.* **38**, 2475–2486 (2015).
7. Verkman, A. S. Does aquaporin-1 pass gas? An opposing view. *J. Physiol.* **542**, 31 (2002).
8. Missner, A. & Pohl, P. 110 Years of the Meyer–Overton rule: predicting membrane permeability of gases and other small compounds. *ChemPhysChem.* **10**, 1405–1414 (2009).
9. Verkman, A. S. Aquaporins at a glance. *J. Cell Sci.* **124**, 2107–2112 (2011).
10. Echevarria, M., Muñoz-Cabello, A. M., Sánchez-Silva, R., Toledo-Aral, J. J. & López-Barneo, J. Development of cytosolic hypoxia and hypoxia-inducible factor stabilization are facilitated by aquaporin-1 expression. *J. Biol. Chem.* **282**, 30207–30215 (2007).
11. Bramley, H. & Tyerman, S. D. Root water transport under waterlogged conditions and the roles of aquaporins in *Waterlogging Signalling and Tolerance in Plants* (ed. Mancuso, S., Shabala, S.) 151–180 (Springer-Verlag, 2010).
12. Springer, B. A. & Sligar, S. G. High-level expression of sperm whale myoglobin in *Escherichia coli*. *Proc. Natl. Acad. Sci. USA* **84**, 8961–8965 (1987).
13. Pemberton, L. F. Preparation of yeast cells for live-cell imaging and indirect immunofluorescence in *Yeast Genetics: Methods and Protocols* (ed. Smith, J. S., Burke, D. J.) 79–90 (Springer, 2014).
14. Emanuelsson, O., Brunak, S., Heijne, G. & Nielsen, H. Locating proteins in the cell using TargetP, SignalP, and related tools. *Nat. Protoc.* **2**, 953–971 (2007).
15. Nakhoul, N. L., Davis, B. A., Romero, M. F. & Boron, W. F. Effect of expressing the water channel aquaporin-1 on the CO<sub>2</sub> permeability of *Xenopus* oocytes. *Am. J. Physiol. Cell Physiol.* **274**, C543–548 (1998).
16. Wang, Y., Cohen, J., Boron, W. F., Schulten, K. & Tajkhorshid, E. Exploring gas permeability of cellular membranes and membrane channels with molecular dynamics. *J. Struct. Biol.* **157**, 534–544 (2007).
17. Hub, J. S. & de Groot, B. L. Mechanism of selectivity in aquaporins and aquaglyceroporins. *Proc. Natl. Acad. Sci. USA* **105**, 1198–1203 (2008).
18. Hub, J. S. & de Groot, B. L. Does CO<sub>2</sub> permeate through aquaporin-1? *Biophys. J.* **91**, 842–848 (2006).
19. Hoque, M. O. *et al.* Aquaporin 1 is overexpressed in lung cancer and stimulates NIH-3T3 cell proliferation and anchorage-independent growth. *Am. J. Pathol.* **168**, 1345–1353 (2006).
20. Wang, J. *et al.* Aquaporins as diagnostic and therapeutic targets in cancer: How far we are? *J. Transl. Med.* **13**, 96 (2015).
21. Wei, X. & Dong, J. Aquaporin 1 promotes the proliferation and migration of lung cancer cell *in vitro*. *Oncol. Rep.* **34**, 1440–1448 (2015).
22. Xie, Y. *et al.* Aquaporin 1 and aquaporin 4 are involved in invasion of lung cancer cells. *Clin. Lab.* **58**, 75–80 (2011).
23. Esteva-Font, C., Jin, B.-J. & Verkman, A. S. Aquaporin-1 gene deletion reduces breast tumor growth and lung metastasis in tumor-producing MMTV-PyVT mice. *FASEB J.* **28**, 1446–1453 (2014).
24. Wu, Z. *et al.* RNAi-mediated silencing of AQP1 expression inhibited the proliferation, invasion and tumorigenesis of osteosarcoma cells. *Cancer Biol. Ther.* **16**, 1332–1340 (2015).
25. Leggett, K. *et al.* Hypoxia-induced migration in pulmonary arterial smooth muscle cells requires calcium-dependent upregulation of aquaporin 1. *Am. J. Physiol. Lung Cell Mol. Physiol.* **303**, L343–353 (2012).
26. Zhang, J. *et al.* AQP1 expression alterations affect morphology and water transport in Schwann cells and hypoxia-induced up-regulation of AQP1 occurs in a HIF-1 $\alpha$ -dependent manner. *Neuroscience* **252**, 68–79 (2013).
27. Govindarajan, S., Hultin, H. O. & Kotula, A. W. Myoglobin oxidation in ground beef: mechanistic studies. *J. Food Sci.* **42**, 571–577 (1977).
28. Xu, H. *et al.* Overexpression of *Laccaria bicolor* aquaporin JQ585595 alters root water transport properties in ectomycorrhizal white spruce (*Picea glauca*) seedlings. *New Phytol.* **205**, 757–770 (2015).
29. Cankorur-Cetinkaya, A. *et al.* A novel strategy for selection and validation of reference genes in dynamic multidimensional experimental design in yeast. *PloS One* **7**, e38351 (2012).
30. Zhao, X. *et al.* A double mutant of sperm whale myoglobin mimics the structure and function of elephant myoglobin. *J. Bio. Chem.* **270**, 20763–20774 (1995).
31. Schenkman, K. A., Marble, D. R., Burns, D. H. & Feigl, E. O. Myoglobin oxygen dissociation by multiwavelength spectroscopy. *J. Appl. Phys.* **82**, 86–92 (1997).
32. Eruslanov, E. & Kusmartsev, S. Identification of ROS using oxidized DCFDA and flow-cytometry in *Advanced Protocols in Oxidative Stress II. Methods in Molecular Biology* (ed. Armstrong, D.) 57–72 (Humana Press, Springer, 2010).
33. Bienert, G. P. *et al.* Specific aquaporins facilitate the diffusion of hydrogen peroxide across membranes. *J. Biol. Chem.* **282**, 1183–1192 (2007).
34. Cole, C. V. & Ross, C. Extraction, separation, and quantitative estimation of soluble nucleotides and sugar phosphates in plant tissues. *Anal. Biochem.* **17**, 526–539 (1966).
35. McElroy, W. D. & DeLuca, M. A. Firefly and bacterial luminescence: basic science and applications. *J. Appl. Biochem.* **5**, 197–209 (1983).

## Acknowledgements

Research funding for this project was provided by the Natural Sciences and Engineering Research Council of Canada and Fundacion Seneca (19631/IV/14 and 19484/PI/14), Murcia, Spain.

## Author Contributions

All authors designed experiments. A.N., H.X. and X.T. performed experiments. J.J.Z., H.X. and X.T. participated in writing the manuscript.

## Additional Information

**Supplementary information** accompanies this paper at <http://www.nature.com/srep>

**Competing financial interests:** The authors declare no competing financial interests.

**How to cite this article:** Zwiazek, J. J. *et al.* Significance of oxygen transport through aquaporins. *Sci. Rep.* **7**, 40411; doi: 10.1038/srep40411 (2017).

**Publisher's note:** Springer Nature remains neutral with regard to jurisdictional claims in published maps and institutional affiliations.



This work is licensed under a Creative Commons Attribution 4.0 International License. The images or other third party material in this article are included in the article's Creative Commons license, unless indicated otherwise in the credit line; if the material is not included under the Creative Commons license, users will need to obtain permission from the license holder to reproduce the material. To view a copy of this license, visit <http://creativecommons.org/licenses/by/4.0/>

© The Author(s) 2017